

Dual emission tuneable in the near-infrared (NIR) and visible (VIS) spectral range by Mix-LnMOF

Roberta Anjos de Jesus ^a, Leonis Lourenço da Luz ^b, Danilo Oliveira Santos ^a, José Arnaldo Santana Costa ^a, Sandro Navickiene ^a, Claudia Cristina Gatto ^c, Severino Alves Júnior ^{b*} and Maria Eliane de Mesquita ^a.

^a Department of Chemistry, UFS, 49100-000, São Cristóvão-SE, Brazil

^b Department of Fundamental Chemistry, UFPE, 50.740-560, Recife – PE, Brazil. Tel. +55 81 2126-7475;
e-mail: salvesjr@ufpe.br

^c University of Brasília (IQ-UnB), campus Universitário Darcy Ribeiro, CEP 70904970, P.O. Box 4478,
Brasília-DF, Brazil.

SUMMARY:

| | |
|-----------------|-------|
| Table S1 ----- | II |
| Table S2 ----- | III |
| Figure S1 ----- | IV |
| Figure S2 ----- | IV |
| Figure S3----- | V |
| Table S3 ----- | V |
| Figure S4----- | VI |
| Figure S5----- | VI |
| Figure S6----- | VII |
| Figure S7----- | VII |
| Figure S8----- | VIII |
| Figure S9----- | VIII |
| Figure S10----- | IX |
| Figure S11----- | IX |
| Figure S12----- | X |
| Figure S13----- | X |
| Figure S14----- | XI |
| Figure S15----- | XI |
| Figure S16----- | XII |
| Figure S17----- | XIII |
| Figure S18----- | XIV |
| Figure S19----- | XV |
| Figure S20----- | XV |
| Figure S21----- | XVI |
| Figure S22----- | XVI |
| Figure S23----- | XVII |
| Figure S24----- | XVII |
| Table S4 ----- | XVIII |
| Figure S25----- | XIX |

Table S1. X-ray diffraction data collection and refinement parameters for **6** and **7**.

| | 7 | 6 |
|---|--|--|
| Chemical formula | C ₂₁ H ₁₆ Nd ₂ N ₃ O _{15.5} | C ₂₁ H ₁₆ Eu ₂ N ₃ O _{15.5} |
| M (g mol ⁻¹) | 846.85 | 862.29 |
| Crystal system | Monoclinic | Monoclinic |
| Space group | P2 ₁ /c | P2 ₁ /c |
| Unit cell <i>a</i> (Å) | 10.975(2) | 10.976(2) |
| <i>b</i> (Å) | 17.469(4) | 17.471(4) |
| <i>c</i> (Å) | 13.387(3) | 13.391(3) |
| β | 101.230(1) | 101.237(1) |
| <i>V</i> (Å ³) | 2517.50(7) | 2518.76(9) |
| <i>Z</i> | 4 | 4 |
| D _c /g cm ⁻³ | 2.234 | 2.274 |
| Index ranges | $-12 \leq h \leq 13$ $-21 \leq k \leq 21$ $-16 \leq l \leq 16$ | $-13 \leq h \leq 13$ $-21 \leq k \leq 21$ $-16 \leq l \leq 13$ |
| Absorption coefficient /mm ⁻¹ | 4.165 | 5.021 |
| Absorption correction | multi-scan | multi-scan |
| Max/min transmission | 0.4622 / 0.3947 | 0.5591 / 0.2723 |
| Measured reflections | 22732 | 26378 |
| Independent reflections / R _{int} | 5160 / 0.0397 | 5151 / 0.0385 |
| Refined parameters | 393 | 388 |
| R1 (F) / wR2 (F ²) (I > 2σ(I)) | 0.0244 / 0.0515 | 0.0295 / 0.0725 |
| GooF | 1.037 | 1.061 |
| Largest diff. peak and hole (eÅ ⁻³) | 0.587 and -0.571 | 0.698 and -0.690 |

$$^a R1 = \sum \|F_o\| - \|F_c\| / \sum \|F_o\|; \quad ^b wR2 = \sqrt{\sum [w(F_o^2 - F_c^2)^2] / \sum [w(F_o^2)^2]}$$

Table S2. Selected bond lengths (Å) and bond angles (°) for (6) and (7).

| (6) | | | | (7) | | | |
|----------------------|-----------|---------------------------------------|-------------|-----------------------|-----------|-------------------------|------------|
| Bonds | (Å) | Atoms | (°) | Bonds | (Å) | Atoms | (°) |
| Eu1-O1 | 2.473(3) | Eu1-O1-Eu ^a | 115.98(11) | Nd1-O1 | 2.554(2) | Nd1-O1-Nd1 ^c | 115.96(9) |
| Eu1-O3 | 2.554(3) | N2-Eu1-N1 | 116.70(11) | Nd1-O3 | 2.474(2) | N2-Nd1-N1 | 116.67(9) |
| Eu1-O3 ^a | 2.550 (3) | O5-Eu1-O1 | 77.32(11) | Nd1-O1 ^c | 2.551 (2) | O5-Nd1-O1 | 154.30(8) |
| Eu1-O5 | 2.444(5) | O11-Eu1-O7 | 140.95(10) | Nd1-O5 | 2.447(2) | O12-Nd1-O7 | 140.92(8) |
| Eu1-O7 | 2.529(3) | O3-Eu1-O13 | 81.36(12) | Nd1-O7 | 2.528(2) | O3-Nd1-O13 | 138.90(10) |
| Eu1-O11 | 2.445(3) | O5-Eu1-O3 | 154.31(10) | Nd1-O12 | 2.444(2) | O5-Nd1-O3 | 77.22(9) |
| Eu1-O13 | 2.554(4) | O5-Eu1-O13 | 73.05(13) | Nd1-O13 | 2.558(3) | O7-Nd1-O1 | 76.57(8) |
| Eu1-N1 | 2.615(4) | O5-Eu1-N2 | 62.81(11) | Nd1-N1 | 2.619(3) | O5-Nd1-N2 | 62.82(9) |
| Eu1-N2 | 2.584(4) | O3-Eu1-N1 | 61.29(10) | Nd1-N2 | 2.581(3) | O7-Nd1-N2 | 61.90(8) |
| Eu2-O2 | 2.346 (3) | O9-Eu2-O10 ^b | 160.97(11) | Nd2-O4 | 2.347 (3) | O9-Nd2-O10 | 161.00(9) |
| Eu2-O8 | 2.376(3) | O2-Eu2-O8 | 153.11(12) | Nd2-O8 | 2.374(3) | O4-Nd2-O8 | 152.93(10) |
| Eu2-O9 | 2.333(3) | O14-Eu2-N3 ^b | 137.94(13) | Nd2-O9 | 2.463(2) | O14-Nd2-N3 | 137.98(10) |
| Eu2-O10 ^b | 2.458 (3) | O9-Eu2-O2 | 100.93(13) | Nd2-O10 | 2.329 (3) | O10-Nd2-O4 | 100.72(11) |
| Eu2-O12 | 2.514(3) | O12-Eu2-O10 ^b | 125.12 (10) | Nd2-O11 | 2.512(2) | O11-Nd2-O9 | 125.21(8) |
| Eu2-O14 | 2.525(4) | O12-Eu2-N3 ^b | 62.33(11) | Nd2-O14 | 2.533(3) | O10-Nd2-O3 | 134.72(9) |
| Eu2-O15 | 2.465(5) | O9-Eu2-O15 | 90.02(19) | Nd2-O15 | 2.474(4) | O4-Nd2-O9 | 89.50(10) |
| Eu2-N3 ^b | 2.565 (4) | O9-Eu2-N3 | 134.74(11) | Nd2-N3 | 2.567 (3) | O9-Nd2-N3 | 62.94(8) |
| Eu1-Eu1 ^a | 4.328(4) | O10 ^b -Eu2-N3 ^b | 62.89(11) | Nd1- Nd1 ^a | 4.328(4) | O11-Nd2-N3 | 62.27(8) |

Simmetry operation: $a = -x+I, -y, -z+2$; $b = x, -y+I/2, z-I/2$; $c = -x+I, -y, -z+I$.

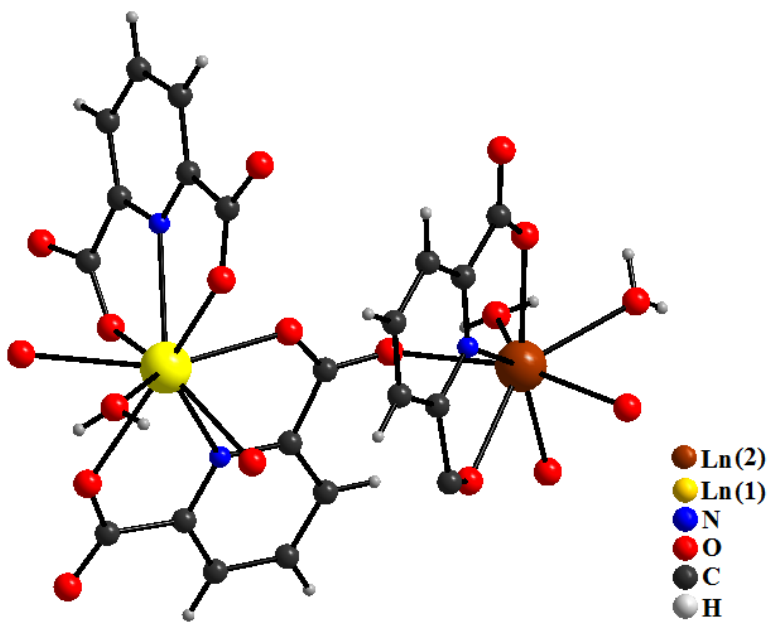


Figure S1: Asymmetric unit from $[\text{Ln}_2(\text{dipc})_3(\text{H}_2\text{O})_3]_n \cdot n\text{H}_2\text{O}$ ($\text{Ln} = \text{Nd}$ and Eu).

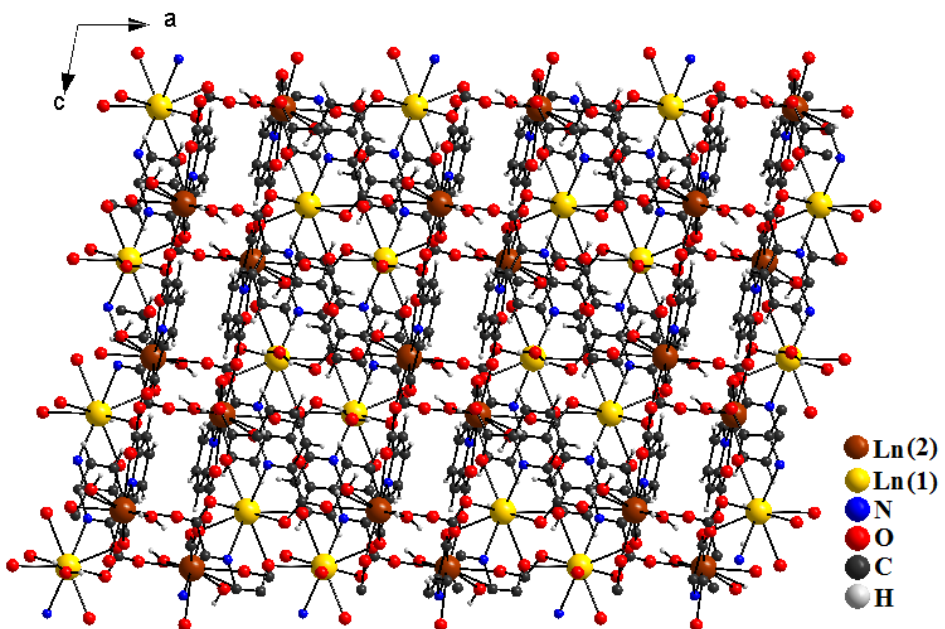


Figure S2: View along the b axis of the extended structure of $[\text{Ln}_2(\text{dipc})_3(\text{H}_2\text{O})_3]_n \cdot n\text{H}_2\text{O}$ material.

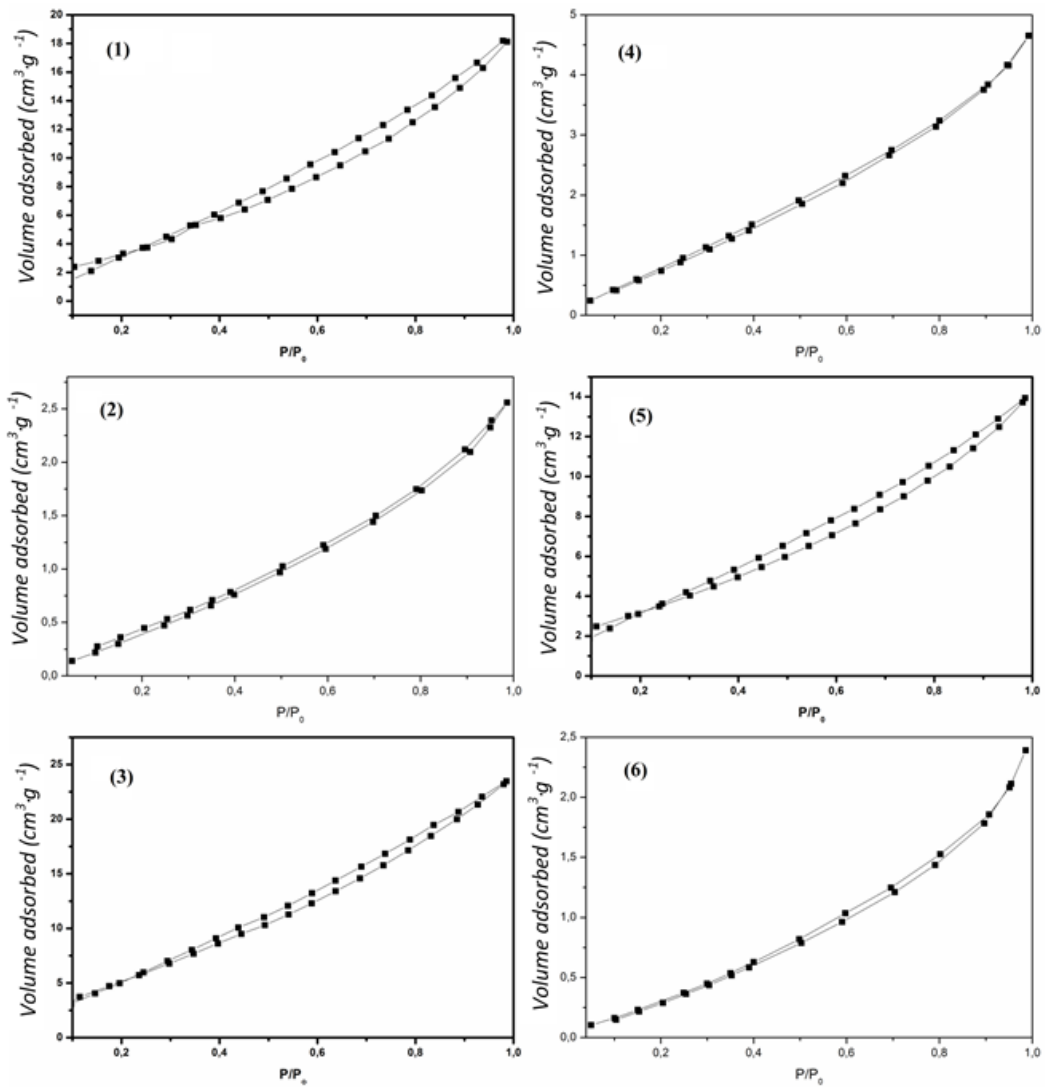


Figure S3. Adsorption – desorption isotherms of nitrogen at 77 K of (1)-(6) compounds.

Table S3: Microporous surface areas.

| Compound | Surface area ($\text{m}^2 \cdot \text{g}^{-1}$) | Pore volume ($\text{cm}^3 \cdot \text{g}^{-1}$) | Pore size (\AA) |
|----------|---|---|----------------------------|
| (1) | 15,996 | 0,027 | 19,112 |
| (2) | 50,140 | 0,048 | 18,060 |
| (3) | 25,820 | 0,032 | 16,894 |
| (4) | 106,50 | 0,086 | 18,020 |
| (5) | 13,515 | 0,019 | 16,980 |
| (6) | 42,670 | 0,045 | 18,120 |

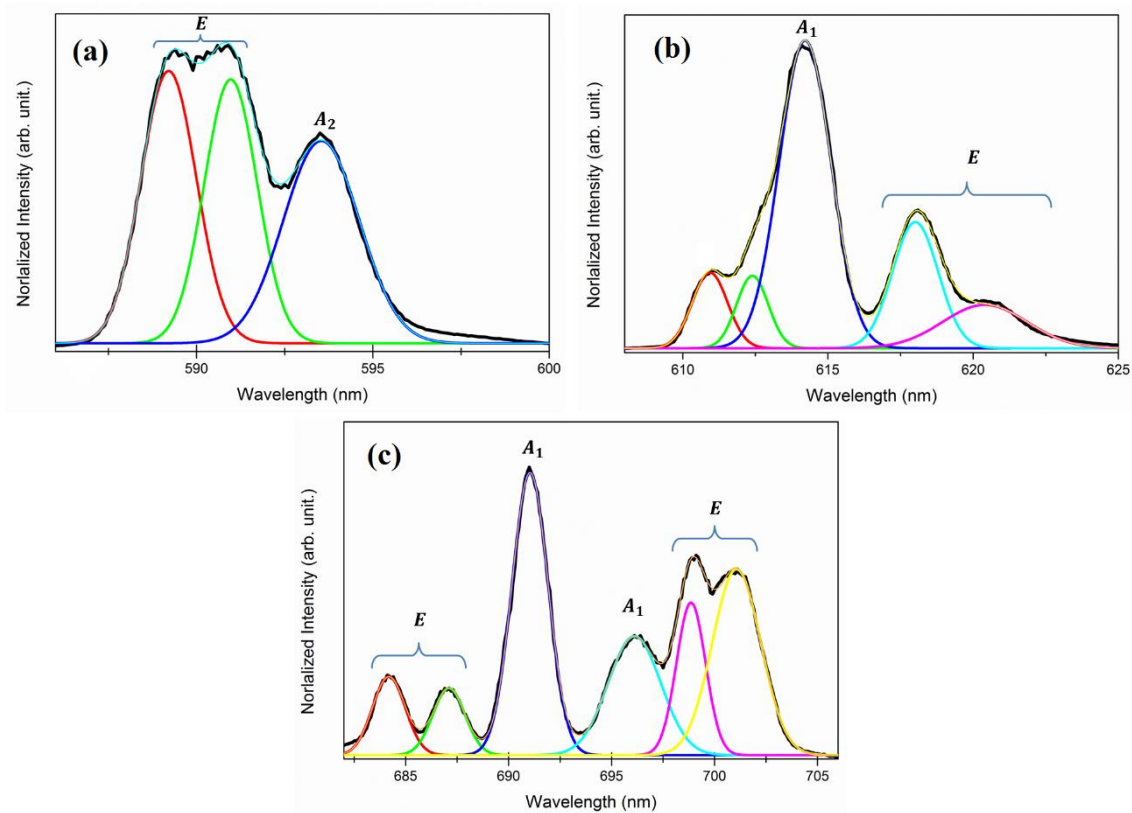


Figure S4: Deconvoluted ${}^5\text{D}_0 \rightarrow {}^7\text{F}_1$ (a), ${}^5\text{D}_0 \rightarrow {}^7\text{F}_2$ (b), and ${}^5\text{D}_0 \rightarrow {}^7\text{F}_4$ (c) transitions of emission spectra from (**6**) compound (10 K) upon excitation at 395 nm (${}^7\text{F}_0 \rightarrow {}^5\text{L}_6$ transition) and irreducible representations of stark components based on C_{4v} symmetry.

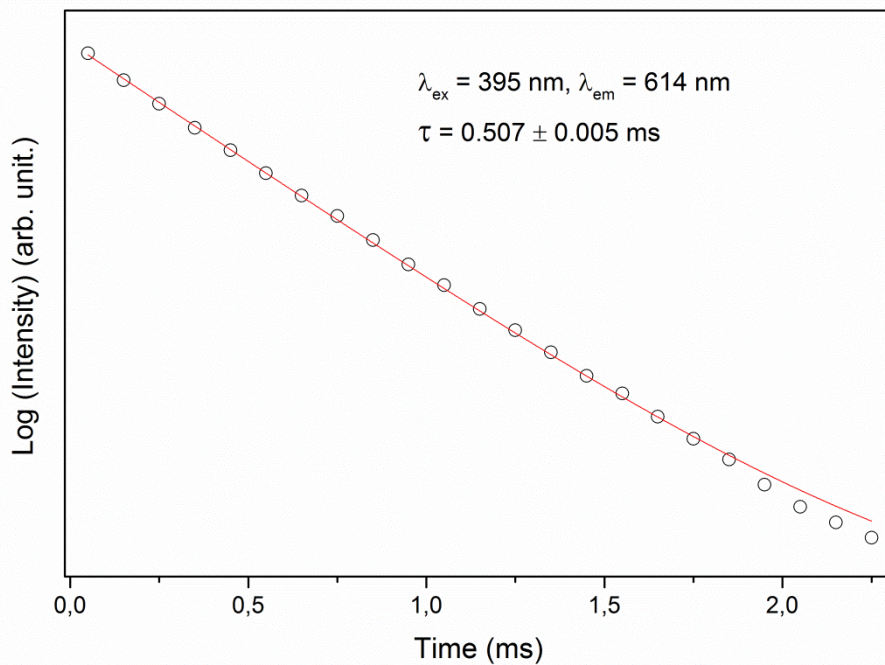


Figure S5: Lifetime of excited state to (**6**) material, upon excitation at 395 nm e monitoring emission at 614 nm (${}^5\text{D}_0 \rightarrow {}^7\text{F}_2$ transition).

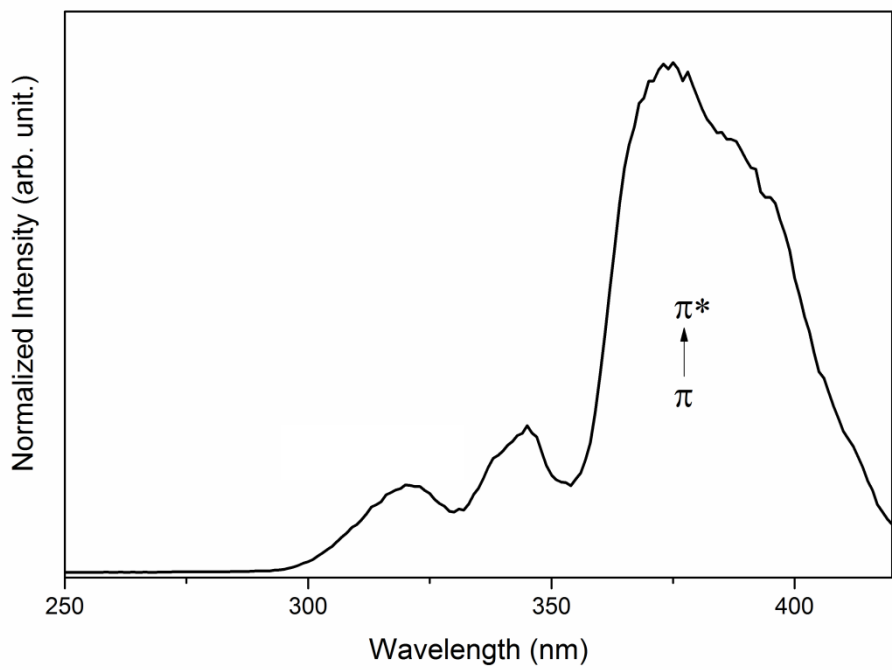


Figure S6: Excitation spectra of (7) material, obtained by monitoring emission at 440 nm ($\pi^* \rightarrow \pi$ transition).

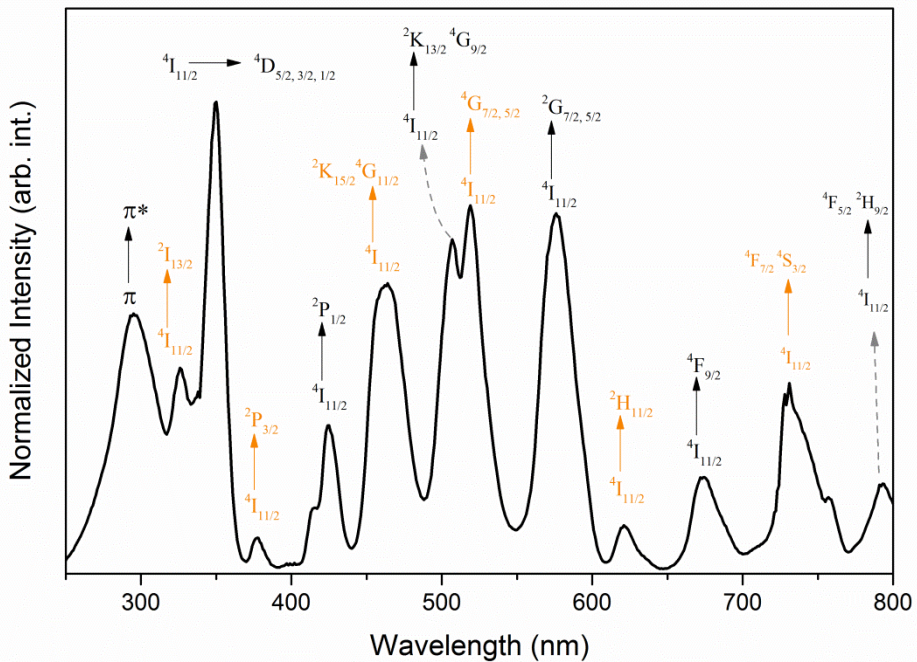


Figure S7: Excitation spectra of (7) material, obtained by monitoring emission at 1060 nm ($^4F_{3/2} \rightarrow ^4I_{11/2}$ transitions).

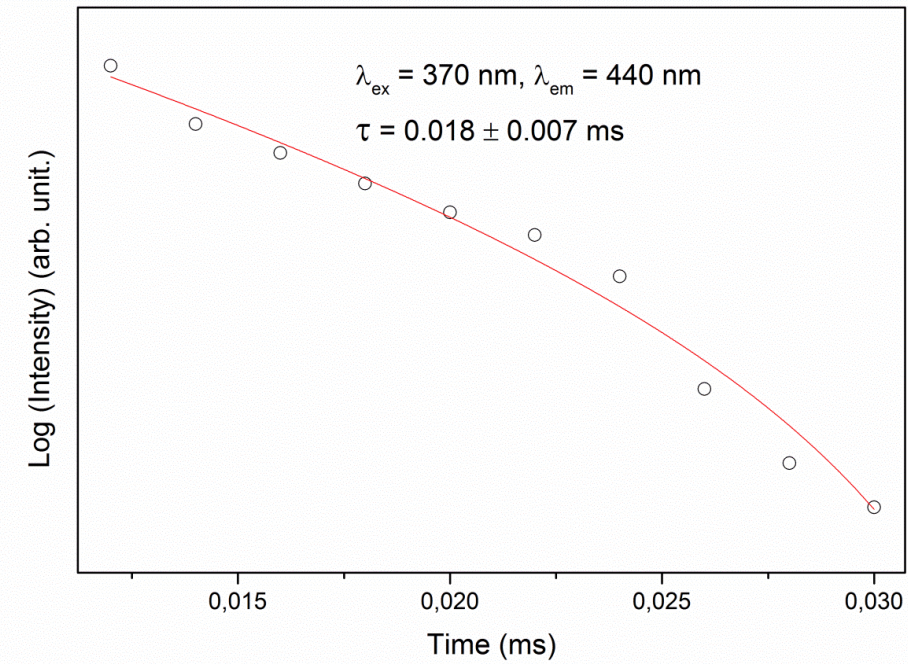


Figure S8: Lifetime of excited state to (7) compound in visible spectral range, upon excitation at 370 nm and monitoring emission at 440 nm ($\pi^* \rightarrow \pi$ transition).

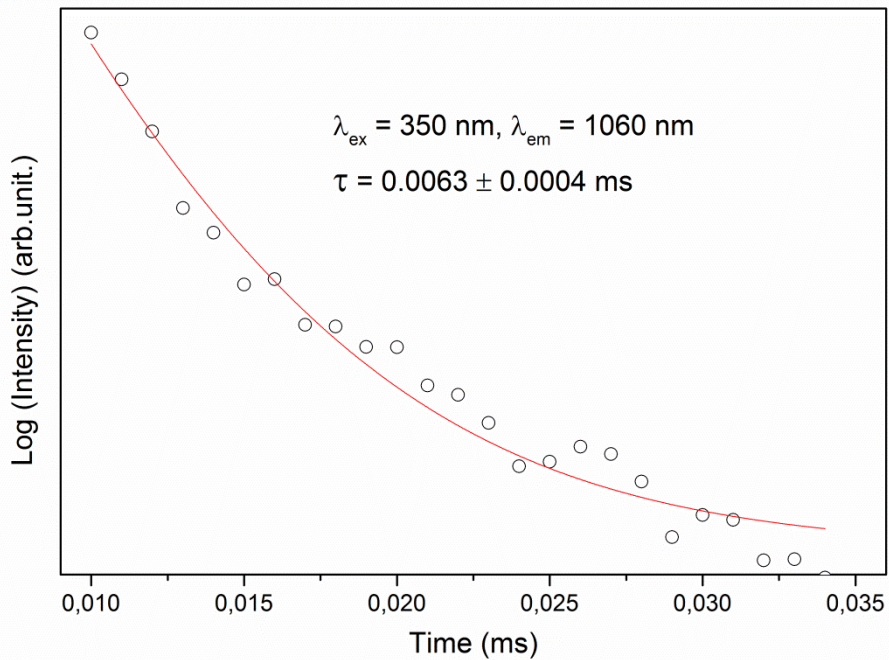


Figure S9: Lifetime of excited state to (7) compound in near-infrared spectral range, upon excitation at 350 nm and monitoring emission at 1060 nm (${}^4\text{F}_{7/2} \rightarrow {}^4\text{I}_{11/2}$ transitions).

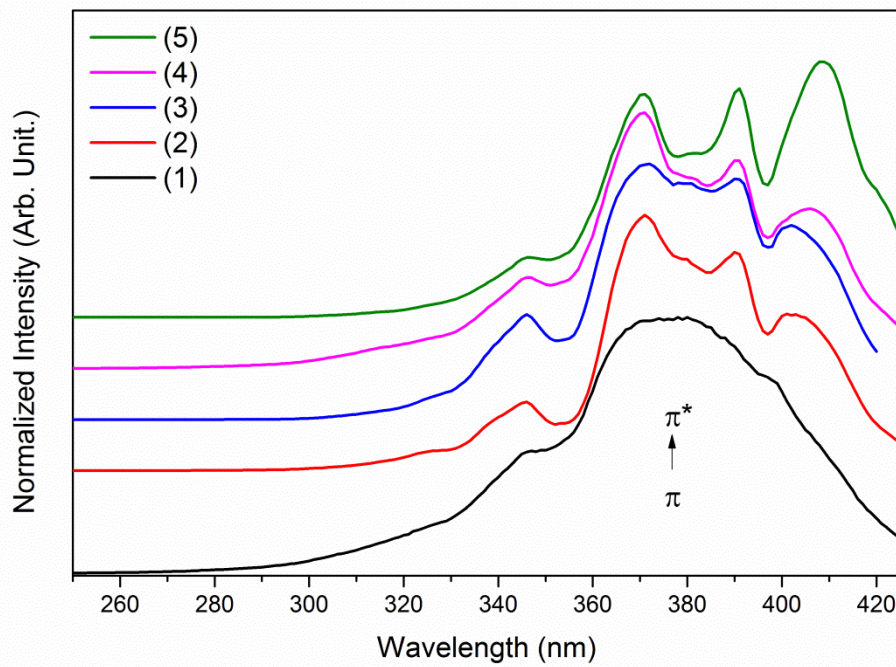


Figure S10: Excitation spectra of (1)-(5) compounds obtained by monitoring emission at 440 nm ($\pi^* \rightarrow \pi$ transition).

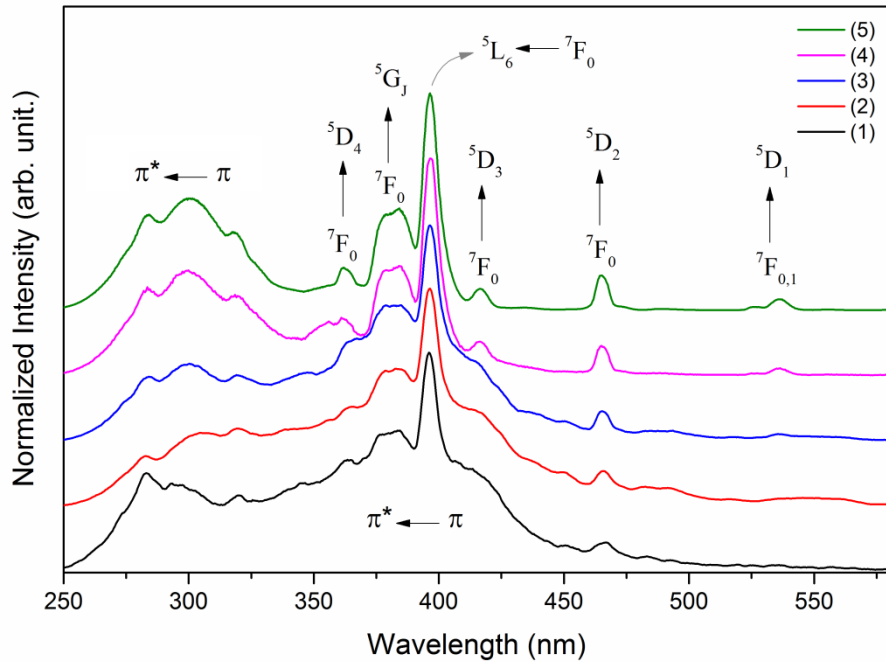


Figure S11: Excitation spectra of (1)-(5) compounds obtained by monitoring emission at 615 nm ($^5D_0 \rightarrow ^7F_0$ transition).

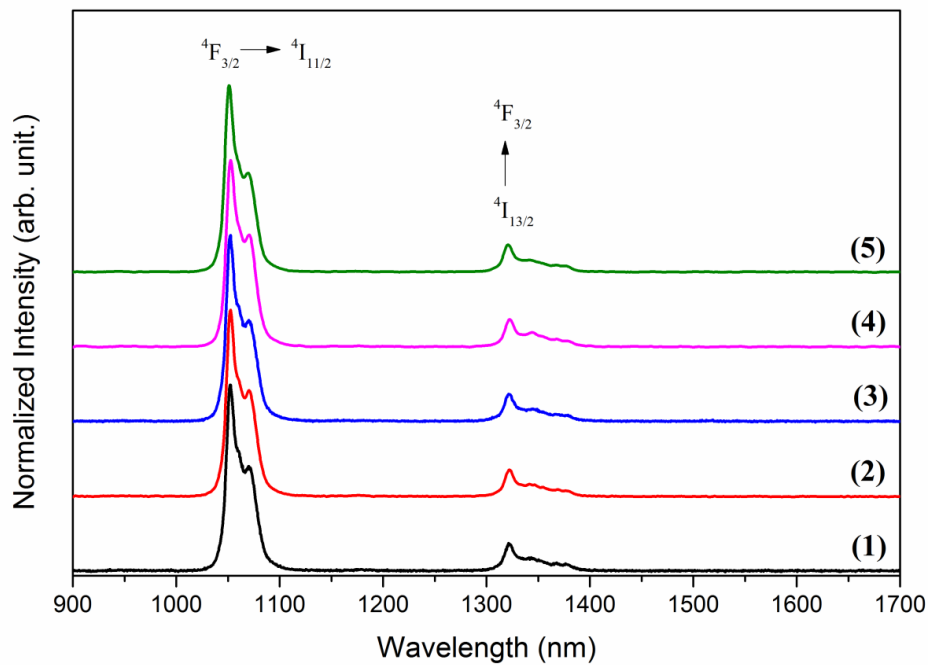


Figure S12: Emission spectra of (1)-(5) compounds upon excitation at 300 nm.

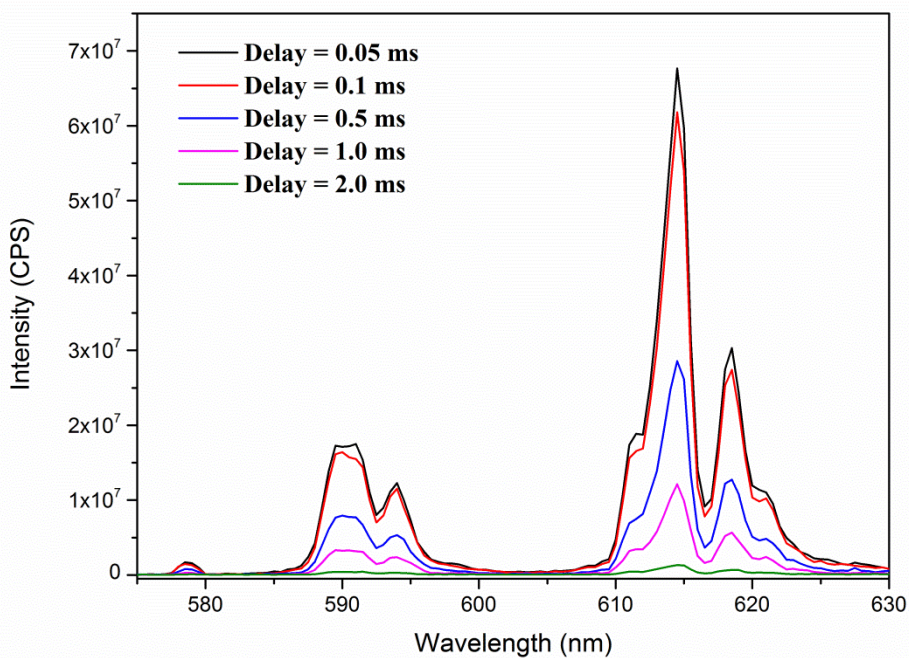


Figure S13: Time resolved emission by excitation at 395 nm of (6) compound

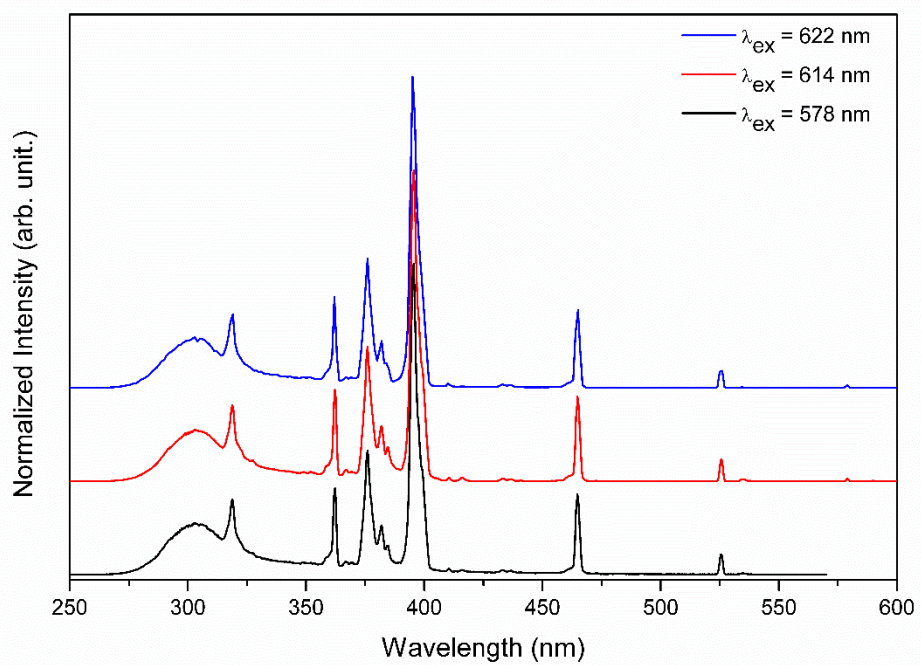


Figure S14: Excitation spectra of (**6**) compound by monitoring emission at 578 ($^5\text{D}_0 \rightarrow ^7\text{F}_0$ transition), 614 and 622 nm ($^5\text{D}_0 \rightarrow ^7\text{F}_2$ transition).

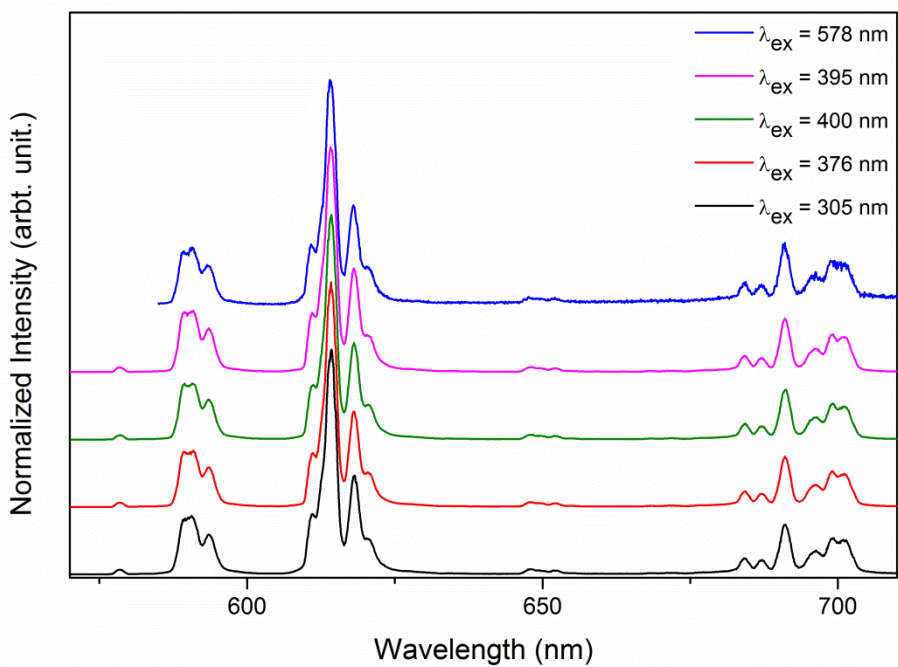


Figure S15: Emission spectra of (**6**) compound by excitation 305 ($\pi \rightarrow \pi^*$ transition), 376 ($^7\text{F}_0 \rightarrow ^5\text{G}_J$ transition), 395 and 400 ($^7\text{F}_0 \rightarrow ^5\text{D}_0$ transition) and 578 nm ($^7\text{F}_0 \rightarrow ^5\text{D}_0$ transition).

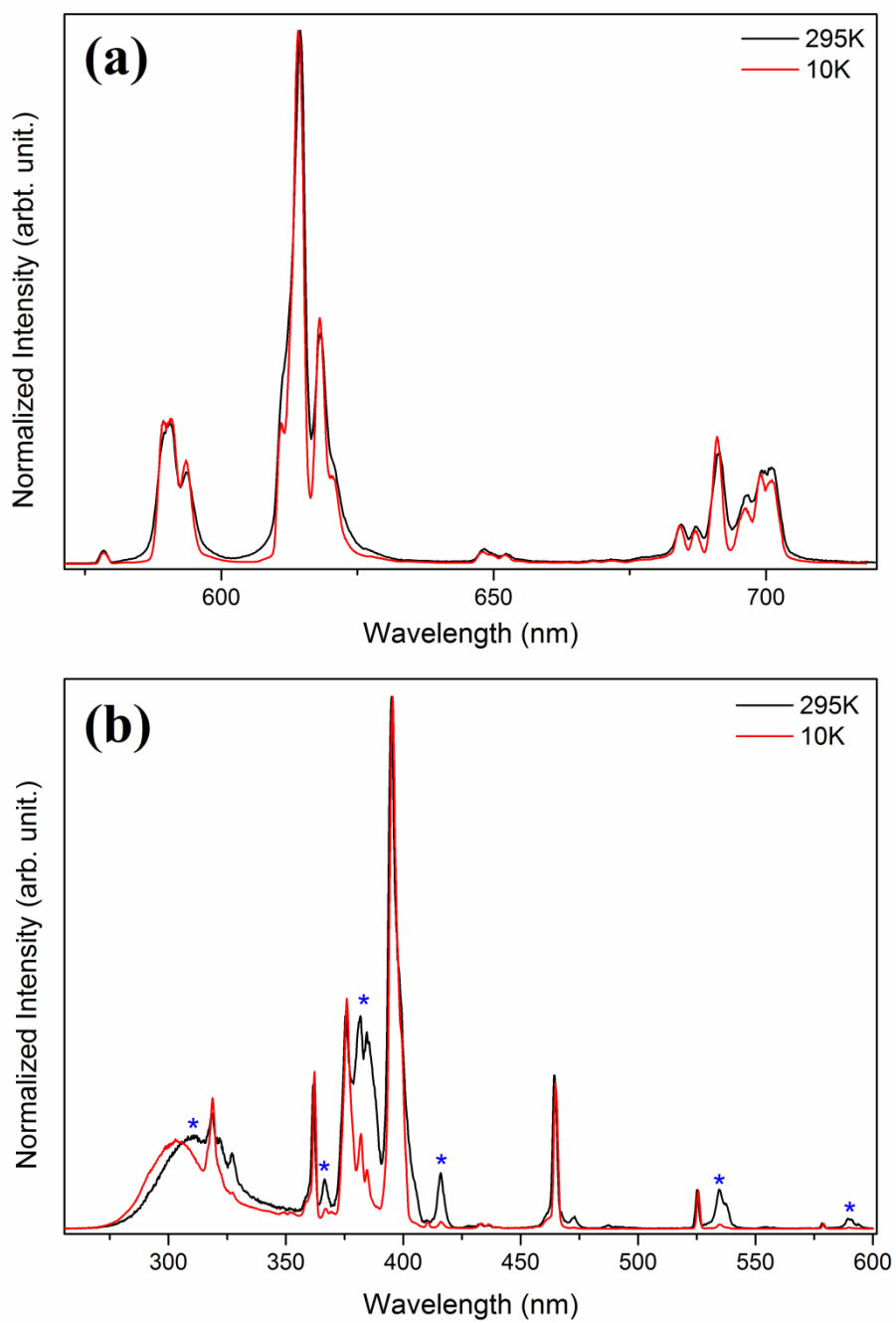


Figure S16: Emission ($\lambda_{\text{ex}} = 395$ nm) and Excitation ($\lambda_{\text{em}} = 615$ nm) spectra of (**6**) compound acquired at 10 (solid red line) and 295 (solid black line) K.

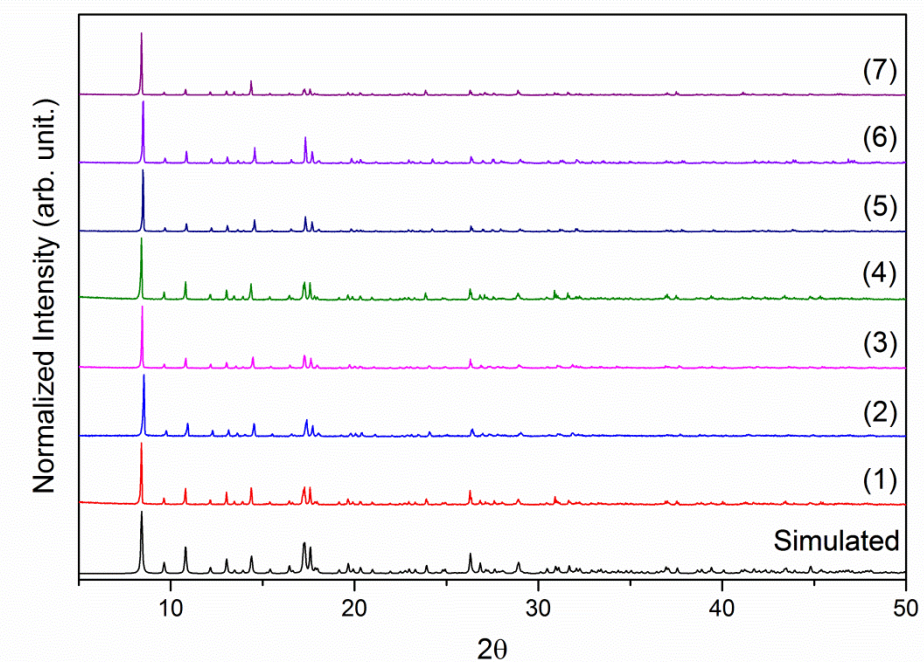


Figure S17: X ray powder diffraction of (1)-(7) materials and simulated.

The absorption spectrum in the infrared from dipc ligand was first reported by Brzsla and Ozga¹ which exhibits two intense and broad band located at 1702 cm^{-1} and 1417 cm^{-1} assigned to the respective asymmetric and symmetric stretches of the C=O bond of carboxylic groups. The vibrations outside C-O bond phase are observed as two bands centered at 1337 cm^{-1} and 1302 cm^{-1} . It can also be observed at 919 cm^{-1} a signal related to the hydrogen bonding carboxylate group, a characteristic band of the deformation out of phase interaction ($\text{OH}\cdots\text{O}$). Since the signal related to vibration of the C=N group of the pyridine ring is located in 1578 cm^{-1} . The presence of small located intensity band $3074\text{-}2540\text{ cm}^{-1}$ may be attributed to stretching of OH bond of carboxyl groups²

From the structural formula of the ligand, can assume that the groups involved in the coordination with the metal carboxylates are the once according to the concepts of Pearson, lanthanide ions are classified as hard acids and preferably with coordinate-hard base. All these bands are shifted to lower energy region formed in the (1)-(7) compounds, indicating coordination with the ligand effect.

The infrared spectra of (1)-(7) coordination polymers, exhibit a broad band from $3340\text{-}3630\text{ cm}^{-1}$ which is related to the presence of water molecules coordinated to the materials. The asymmetric stretching band of the C=O bond and vibrations outside C-O bond phase of the carboxylic groups, located at 1702 cm^{-1} and, 1337 cm^{-1} and 1302 cm^{-1} , respectively, in the free ligand. This values was shifted to higher and lower

frequencies for C=O and C-O bond, respectively, in the all coordination polymers. The web stretch associated with the C=N of the pyridine ring was found to be slightly shifted to lower frequencies at 1544 cm^{-1} complex in (1)-(7) compounds, compared with its original position at 1578 cm^{-1} in the free ligand, indicating coordination of Eu^{3+} and Nd^{3+} ions via carboxylate oxygen atoms and nitrogen atoms in the pyridine ring present in the ligand. These data were corroborated by further data obtained by single crystal crystallography of $[(\text{Nd}_{1-x}\text{Eu}_x)_2(\text{dipc})_3(\text{H}_2\text{O})_3]_n \cdot n\text{H}_2\text{O}$ ($x = 0, 0.1, 0.3, 0.5, 0.7, 0.9$ and 1) materials.

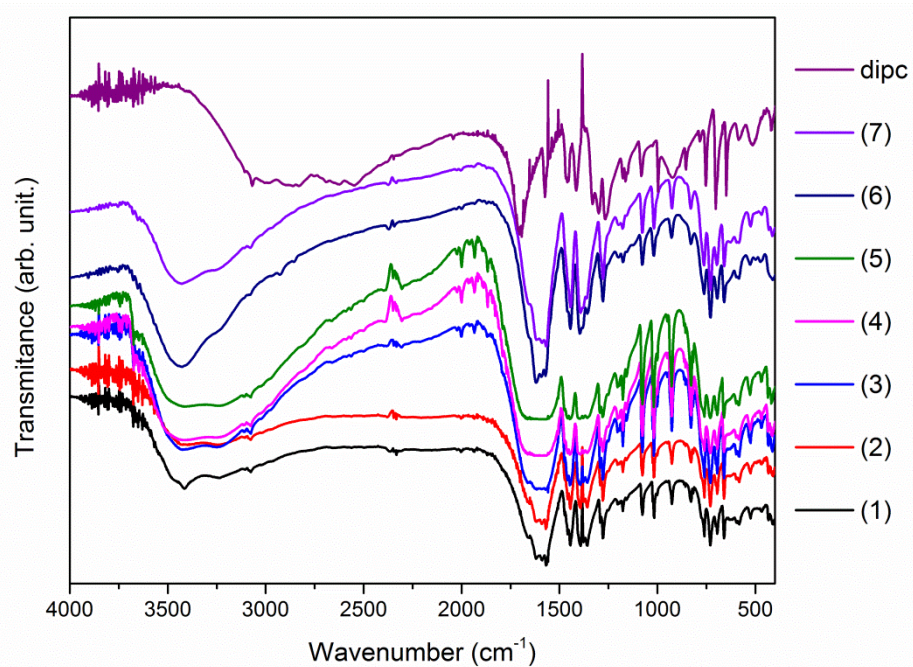


Figure S18: IR spectra of (1)-(7) materials and dipc ligand.

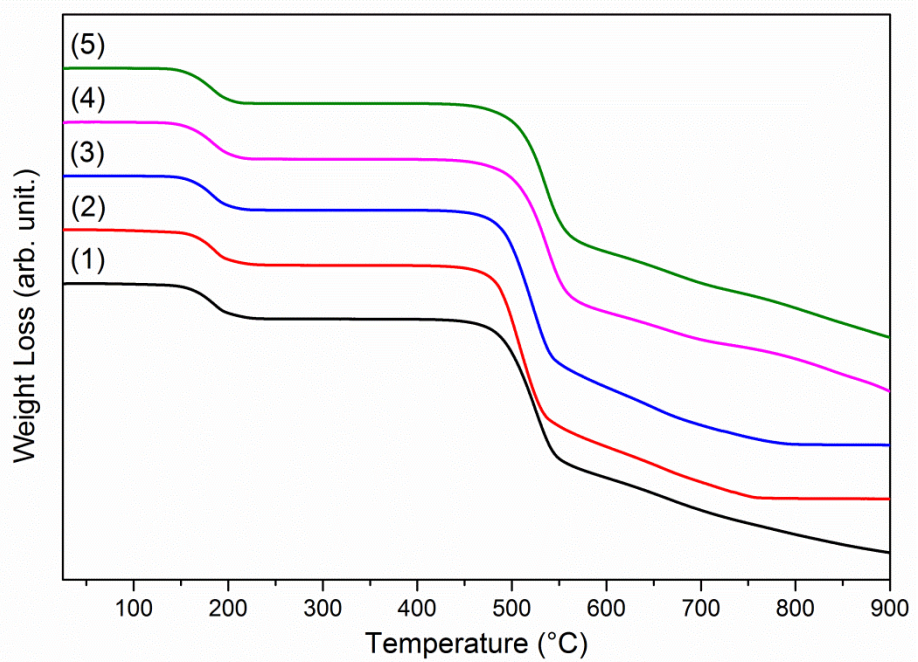


Figure S19: Thermal stability of (1)-(5) materials.

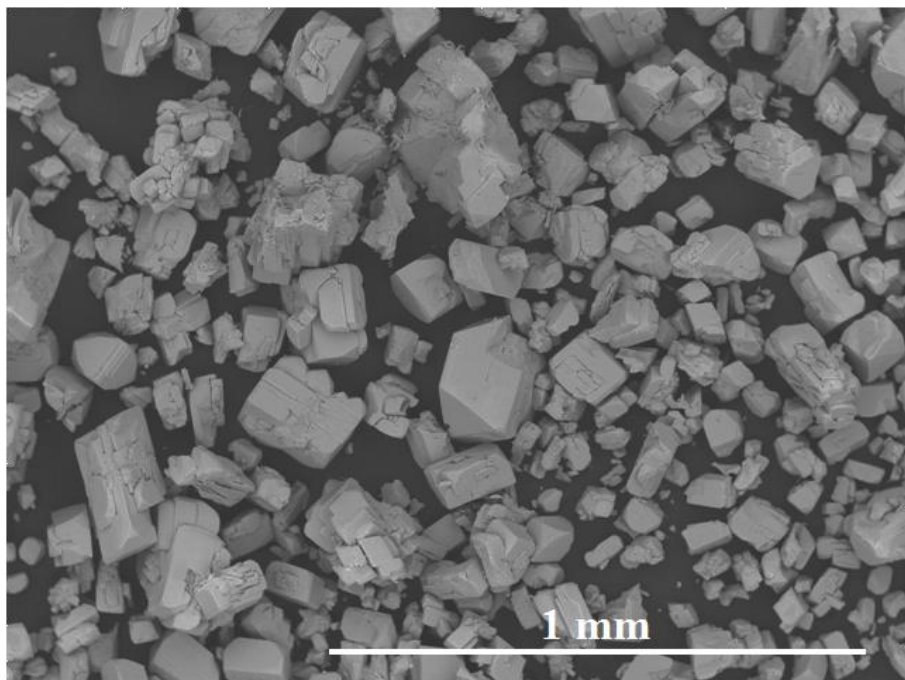


Figure S20: SEM images of (1) at x100 of magnification

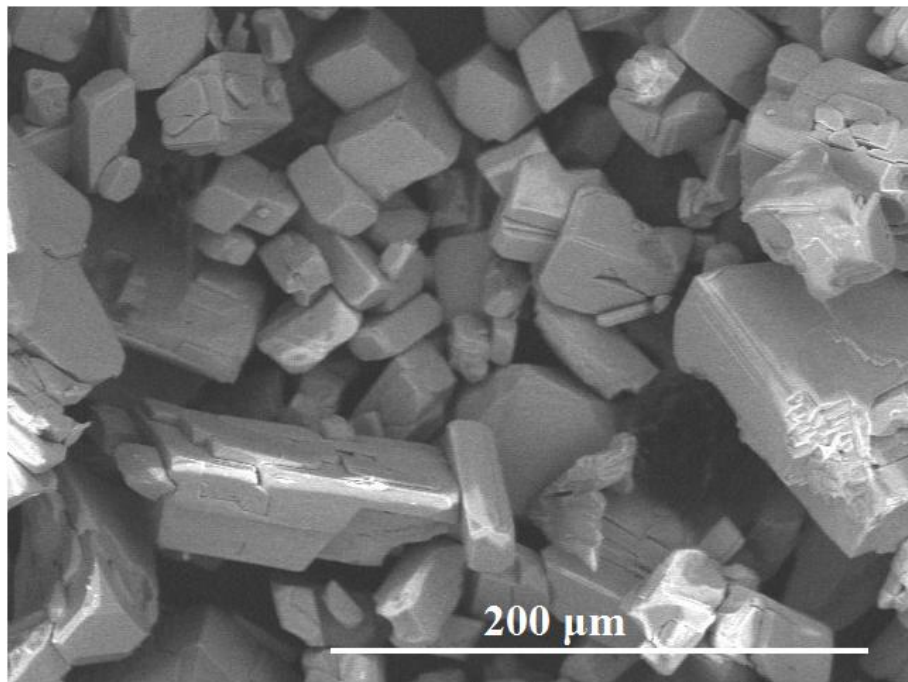


Figure S21: SEM images of (2) at x500 of magnification.

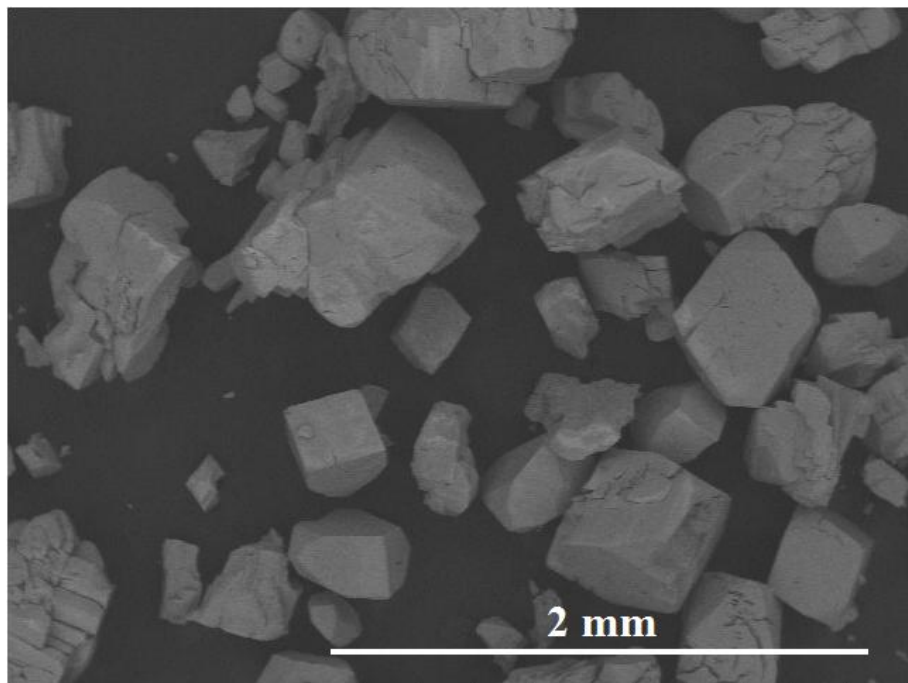


Figure S22: SEM images of (3) at x50 of magnification

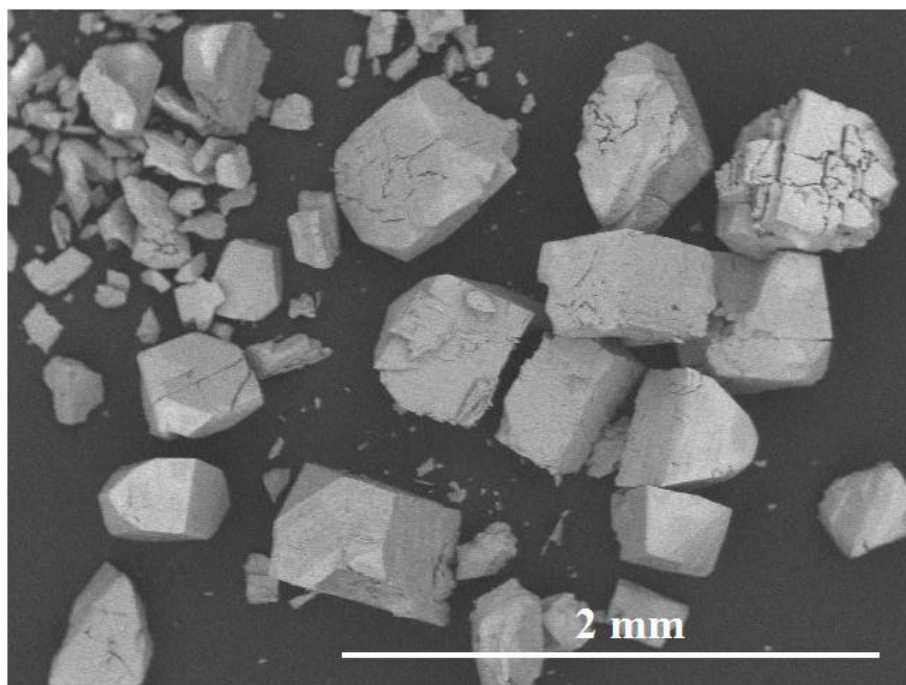


Figure S23: SEM images of (4) at x50 of magnification.

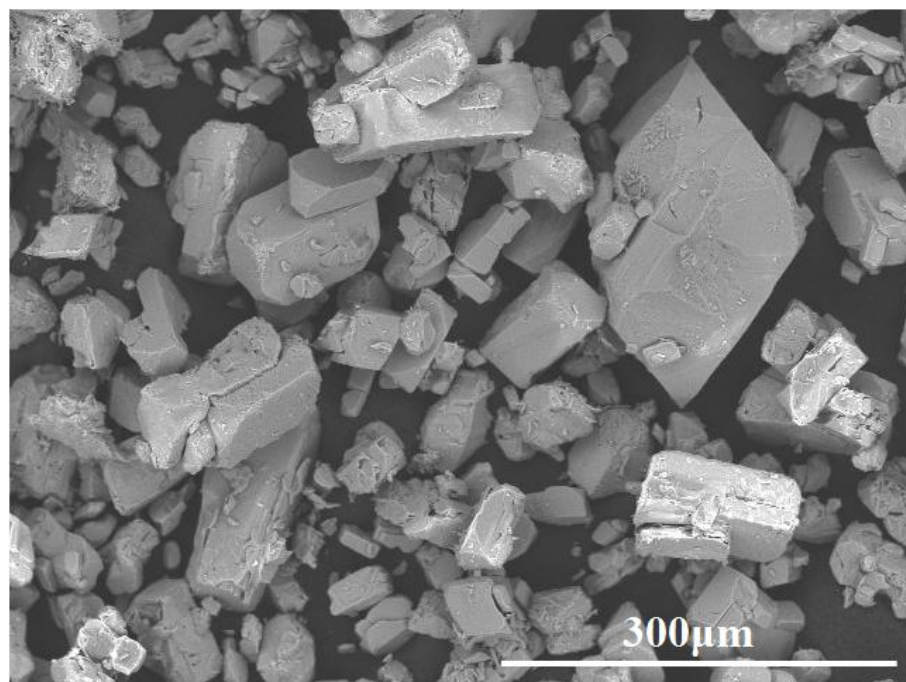


Figure S24: SEM images of (5) at x250 of magnification.

Table S4: EDX elemental analyze

| MOF | <i>Eu (%)</i> | <i>Nd (%)</i> |
|------------|----------------------|----------------------|
| (1) | 8.99 | 91.00 |
| (2) | 28.97 | 68.99 |
| (3) | 48.01 | 51.90 |
| (4) | 70.99 | 31.06 |
| (5) | 88.79 | 11.20 |
| (6) | 96.58 | - |
| (7) | - | 100.0 |

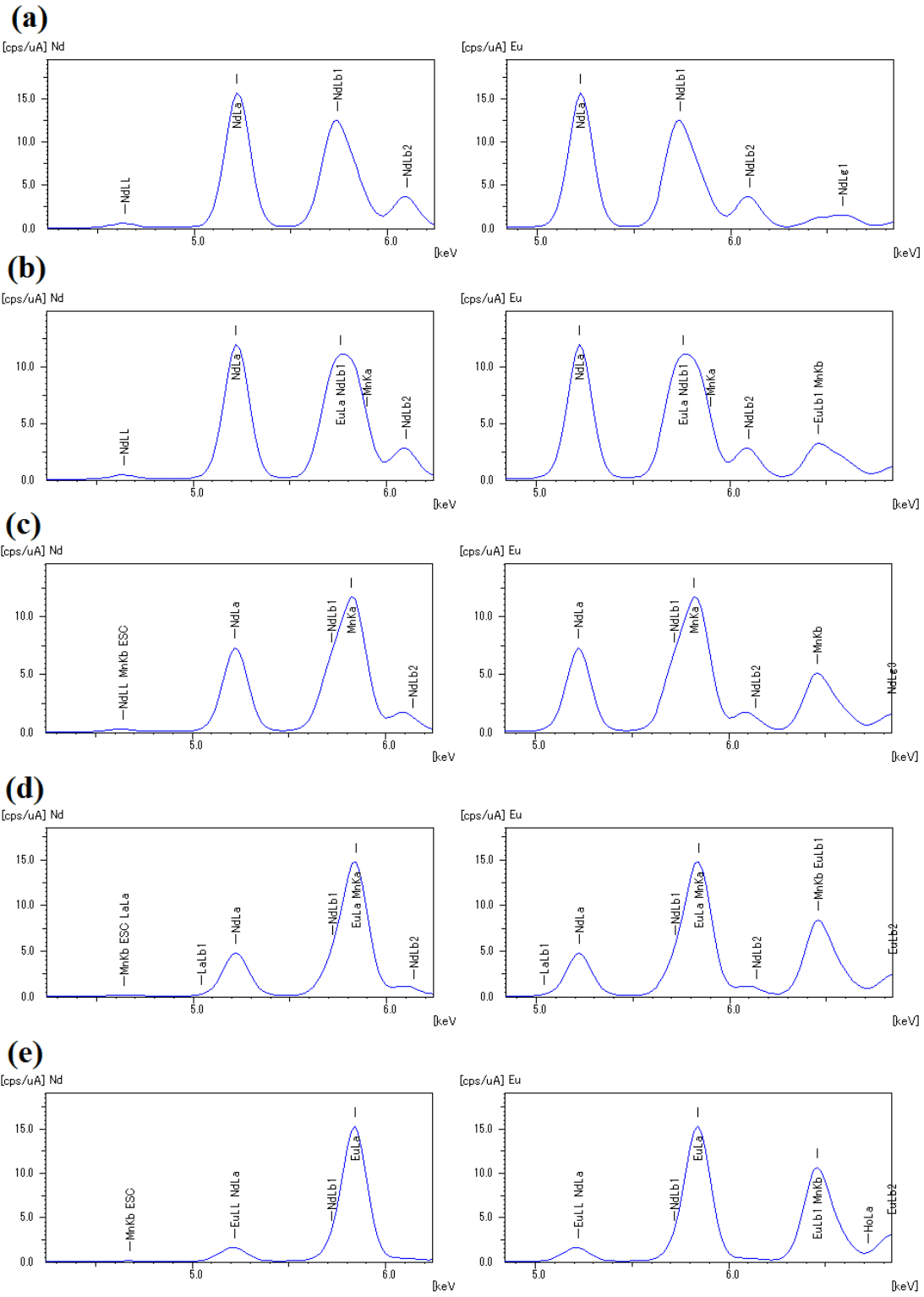


Figure S25: EDX spectra of (1)-(5) compounds, respectively to (a)-(e)

References

- ¹ Brzyska, W.; Ozga, W. Preparation and Properties of Rare Earth Element Complexes with Pyridine-2,6-dicarboxylic Acid. *Thermochimica Acta*, v. 247, p. 329-339, 1994.
- ² Gonzalez-Baró, A. C.; Castellano, E. E.; Piro, O. E.; Parajón-Costa, B. S. Synthesis, Crystal Structure and Spectroscopic Characterization of a Novel Bis (Oxo-Bridged) Dinuclear Vanadium(V)-Dipicolinic Acid Complex. *Polyhedron*, v. 24, p. 49-55, 2005.